ACS Catalysis

Research Article

pubs.acs.org/acscatalysis

Bioinspired Complex-Nanoparticle Hybrid Catalyst System for Aqueous Perchlorate Reduction: Rhenium Speciation and Its Influence on Catalyst Activity

Jinyong Liu,[†] Jong Kwon Choe,[†,¶] Yin Wang,[†,§] John R. Shapley,[‡] Charles J. Werth,[†,⊥] and Timothy J. Strathmann*[,†]

[†]Department of Civil and Environmental Engineering and [‡]Department of Chemistry, University of Illinois at Urbana−Champaign, Urbana, Illinois 61801, United States

Supporting Information

ABSTRACT: A highly active catalyst for reduction of the inert water contaminant perchlorate (ClO_4^-) to Cl^- with 1 atm H_2 at 25 °C is prepared by noncovalently immobilizing the rhenium complex $Re^V(O)(hoz)_2Cl$ (hoz = 2-(2′-hydroxyphenyl)-2-oxazoline) together with Pd^0 nanoparticles on a porous carbon support. Like the Mo complex centers in biological oxyanion reductases, the immobilized Re complex serves as a single site for oxygen atom transfer from ClO_4^- and ClO_x^- intermediates, whereas Pd^0 nanoparticles provide atomic hydrogen reducing equivalents to sustain redox cycling of the immobilized Re sites, replacing the more complex chain of electron transfer steps that sustain Mo centers within oxyanion reductases. An in situ aqueous adsorption method of immobilization was used to preserve the active $Re^V(O)(hoz)_2$ structure during bimetallic catalyst preparation and enable study of Re redox cycling and reactions with ClO_4^-. Heterogeneous reaction kinetics, X-ray photoelectron spectroscopy, and experiments with homogeneous model Re complexes are combined to obtain insights into the catalytic reaction mechanisms and the influence of Re speciation on catalyst reactivity with ClO_4^-. Redox cycling between hoz-coordinated Re^V and Re^{VII} species serves as the main catalytic cycle for ClO_4^- reduction. Under reducing conditions, approximately half of the immobilized hoz-coordinated Re^V is further reduced to Re^{III}, which is not directly reactive with ClO_4^-. A small fraction of the hoz-coordinated Re^{VII} species can dissociate to ReO_4^- and free hoz, which are then reductively reimmobilized as a less reactive mixture of Re^V, Re^{III}, and Re^I species. This study provides an example wherein highly active metal complexes that were originally developed for homogeneous organic phase catalysis can be incorporated into heterogeneous catalysts for practical environmental applications. Findings suggest a general blueprint for developing hybrid catalysts combining single-site transition metal complexes with hydrogen-activating metal nanoparticles.

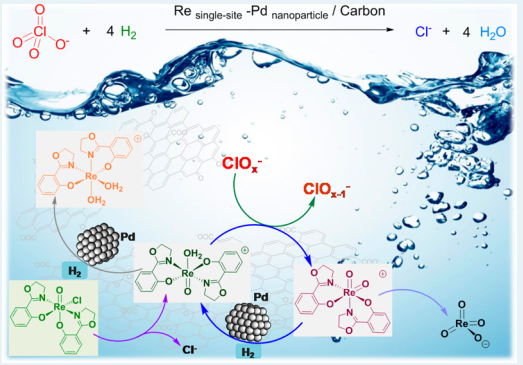

KEYWORDS: *perchlorate, rhenium, palladium, bimetallic catalyst, oxygen atom transfer, water treatment, environmental remediation, X-ray photoelectron spectroscopy*

INTRODUCTION

Growing scarcity of high-quality drinking water supplies across the globe heightens the need for innovative and sustainable technologies for drinking water decontamination and wastewater reuse.[1−4] Perchlorate (ClO_4^-), a chemically inert but toxic oxyanion, has been widely detected in water supplies[5,6] and agricultural products[7,8] as a result of source water contamination from improper disposal of explosive materials, use of contaminated fertilizers, and natural atmospheric formation processes.[9−11] Excess exposure to ClO_4^- disrupts iodide uptake by the thyroid gland, affecting hormone levels and metabolism, especially in developing fetuses and young children.[12,13] In 2011, the U.S. EPA announced plans to set a national drinking water standard for ClO_4^-.[14] Several ClO_4^- contamination incidents have recently caused drinking water supply interruption in California,[15] highlighting the need for developing effective technologies to remove ClO_4^- and related recalcitrant oxyanion contaminants (e.g., ClO_3^-, NO_3^-, CrO_4^{2-}) from water.

Complete chemical reduction (e.g., reaction with Fe^0, Fe^{2+}, or Ti^{3+}) of ClO_4^- to the innocuous Cl^- in water generally requires harsh conditions (e.g., high temperature) and a large excess concentration of reductants.[16−20] In sharp contrast, a number of bacteria efficiently grow under ambient conditions by coupling oxidation of organic or inorganic electron donors (e.g., formate, acetate, ethanol, H_2, H_2S) with the reduction of ClO_4^- or NO_3^-.[13] In nitrate reductases (e.g., NarG−NarH−NarI in *Escherichia coli*; perchlorate reductase is very similar, but

Received: August 28, 2014
Revised: December 6, 2014
Published: December 9, 2014

DOI: 10.1021/cs501286w
ACS Catal. 2015, 5, 511−522

the structure has not been fully characterized), a Mo−bisMGD complex (biosynthesized from MoO_4^{2-}, MGD = molybdopterin guanine dinucleotide) in the NarG subunit acts as the highly active site for NO_3^- reduction to NO_2^-.[21,22] Redox cycling of the Mo complex is maintained by a series of electron-transfer processes involving a pair of heme complexes in the NarI subunit and a series of [Fe−S] clusters in the NarH subunit (Figure 1a). In addition, electron transfer from the exogenous

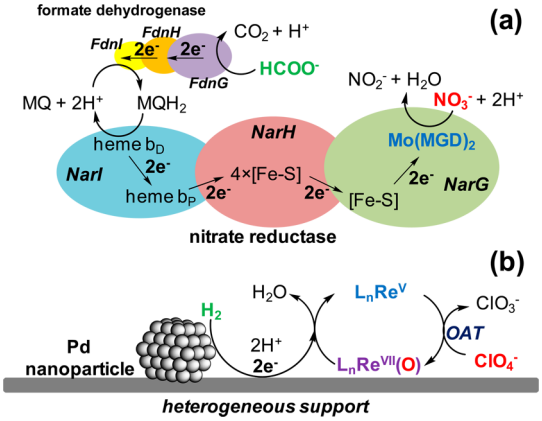

Figure 1. Simplified illustration of electron transfer for oxyanion reduction by (a) nitrate-reducing *E. coli* enzymes and (b) perchlorate-reducing Re−Pd/C catalysts.

electron donors to the reductase enzyme involves a series of other metalloenzymes (e.g., formate dehydrogenase FdnG−FdnH−FdnI) and electron shuttles (e.g., quinol, NADH and NADPH).[22,23] For perchlorate reduction, perchlorate reductase reduces ClO_4^- to ClO_3^- via Mo-catalyzed oxygen atom transfer (OAT) reactions, then a second enzyme, chlorite dismutase, is employed to complete the transformation of ClO_3^- to Cl^- and O_2.[13]

Inorganic chemists have identified oxo species of Mo^{VI}, W^{VI}, Re^{VII}, Ru^{VI}, and Os^{VI} as homogeneous catalyst precursors for ClO_4^- reduction.[24−28] OAT from ClO_4^- to reduced oxophilic metal species (e.g., Re^{V}, Ru^{III}, Os^{IV})[29] triggers the stepwise reduction of ClO_4^- to Cl^-. Abu-Omar and co-workers[30] reported the highest reactivity for ClO_4^- at ambient temperature using an oxorhenium complex, $[Re(O)(hoz)_2]^+$ (hoz = 2-(2′-hydroxyphenyl)-2-oxazoline, a naturally occurring structure in microbial siderophores),[31] as a homogeneous catalyst in CH_3CN. However, the concentrated acids (e.g., 1−10 M HCl, HOTf or H_2SO_4), toxic reducing agents (e.g., HBr, $SnCl_2$, H_3PO_2, organic sulfides) and the organic solvent (e.g., CH_3CN for Re complex) used in these studies are incompatible with water purification applications. At the same time, hydrogenation metals (e.g., Pd^0, Ni^0, Pt^0) have been shown to catalyze the reduction of more reactive oxyanion contaminants (e.g., BrO_3^-, NO_2^-) using H_2,[32] but these metallic hydrogenation catalysts show little reactivity with ClO_4^- in water.[33]

To address the limitations of the individual homogeneous and heterogeneous catalyst systems, a synthetic bimetallic catalyst inspired by the biological reductase system was designed by combining Pd^0 nanoparticles with $[Re(O)(hoz)_2]^+$ complexes on an activated carbon support (i.e., $Re(hoz)_2$−Pd/C) for highly active reduction of aqueous ClO_4^-. The hybrid catalyst utilizes the high OAT activity of the synthetic Re complex and simplifies the electron transfer process in comparison to biological systems. Pd-activated hydrogen directly provides electrons to sustain redox cycling of the immobilized Re complex for ClO_4^- reduction (Figure 1b). This contribution describes the preparation, performance, and mechanistic characterization of the $Re(hoz)_2$−Pd/C catalyst. In contrast with previous efforts,[34] an in situ aqueous deposition method performed in the presence of a reducing headspace gas (H_2) was employed to prevent decomposition of the active Re complex during immobilization on the carbon support. This yielded a catalyst that exhibits a much higher activity for ClO_4^- reduction than other heterogeneous catalysts, including a Re−Pd/C catalyst prepared from the same $Re(O)(hoz)_2Cl$ precursor complex by incipient wetness impregnation under air[34] and catalysts prepared from alternative Re precursors.[35−38] Beyond the kinetics measurements, efforts were undertaken to characterize Re speciation at the heterogeneous catalyst surface under varying solution conditions, providing new mechanistic insights into surface redox processes that control catalyst stability and reactivity with oxyanions, including formation of previously unreported Re^{III} surface species. Parallels to the biological reductase system are discussed, and strategies for further enhancing catalyst activity and stability through targeted modification of the Re coordination structure are suggested.

EXPERIMENTAL SECTION

General Information. All chemicals were obtained from commercial suppliers and used as received. The 5 wt % Pd/C (Sigma-Aldrich, Degussa type E101 NO/W wet support) was wet-sieved to obtain the <37 μm fraction, dried under air at 110 °C for 2 h and heated under H_2 flow at 250 °C for 1 h. The surface area (892 $m^2\ g^{-1}$) and pore volume (0.235 $cm^3\ g^{-1}$) of Pd/C were measured by N_2 adsorption/desorption at 77 K (Micromeritics ASAP 2010). The size of immobilized Pd nanoparticles ranged from 1.5 nm to >8 nm (4 nm on average), as previously characterized.[34] Aqueous solutions were prepared using deionized (DI) water (Barnstead Nanopure system; resistivity >17.5MΩ cm). Ultrahigh purity H_2 gas (99.999%, Matheson) was used to sparge aqueous catalyst suspensions.

Re Compound Synthesis and Homogeneous Reaction Experiments. Synthesis procedures and characterization data for Hhoz ligand and hoz-coordinated Re^{V} and Re^{III} compounds are provided in the Supporting Information. Homogeneous reaction kinetics between Re complexes and $LiClO_4$ dissolved in CD_3CN were measured by ^1H−NMR and ^{31}P−NMR. Full details of these experiments are provided in the Supporting Information.

Preparation of $Re(hoz)_2$−Pd/C Catalyst. $Re(hoz)_2$−Pd/C catalysts were prepared from Pd/C and synthesized $Re(O)(hoz)_2Cl$ using two different procedures described in the following.

Procedure A (Aqueous Adsorption). A 50 mL pear-shaped flask was sequentially loaded with 3.8 mg of $Re(O)(hoz)_2Cl$, 25 mg of Pd/C, and a magnetic stir bar. The flask was manually shaken to physically mix the two powders together, and then 50 mL of water (pH 3, by addition of 1 mM HCl) was added. The flask was sealed with a rubber stopper and sonicated for 2 min with occasional shaking. The flask was then placed in a 25 °C water bath and sparged with H_2 through two stainless steel needles that penetrated the stopper and served as gas inlet and outlet (through a silicon oil bubbler vented to a fume hood atmosphere), respectively. The suspension was stirred at 1100 rpm under 1 atm H_2 for 4 h to allow adequate time for transfer of the Re complex from the bulk powder to the activated

DOI: 10.1021/cs501286w
ACS Catal. 2015, 5, 511−522

carbon matrix. This yielded a typical 0.5 g L^{-1} suspension of $Re(hoz)_2$–Pd/C catalyst containing nominally 5 wt % Re and 5 wt % Pd.

Procedure B (Incipient Wetness). For the same materials loading in the 50 mL scale experiment described above, in an anoxic atmosphere (~99% N_2 and ~1% H_2 glovebox; Coy Laboratories) the $Re(O)(hoz)_2Cl$ was dissolved in 0.6 mL of CH_2Cl_2 and added dropwise to the Pd/C powder in multiple portions. Each portion of the solvent was removed by vacuum before adding the next. Deoxygenated water (pH 3) and a magnetic stir bar were then added, and the flask was sealed by a rubber stopper and removed from the glovebox. After sonication for 2 min, H_2 sparging was initiated, and the flask was placed in the 25 °C water bath to prepare for reaction with ClO_4^-.

Preparation of Other Re–Pd/C Catalysts. The ReO_x–Pd/C catalyst was prepared from reductive immobilization of ReO_4^- in Pd/C, as described elsewhere.[36] Briefly, a 50 mL flask was loaded with 25 mg of Pd/C and 50 mL of aqueous solution containing 1 mM HCl and 0.134 mM NH_4ReO_4. After sonication for 1 min, the flask was sealed and placed in a 25 °C water bath and sparged with H_2 for 12 h to ensure reductive immobilization of the ReO_4^-.[38] For ligand-enhanced ReO_x–Pd/C catalysts, ReO_4^- was added together with the desired ligand (4-dimethylaminopyridine, Hhoz or 2-methyloxazoline) at a 1:2 molar ratio to the Pd/C suspension before H_2 sparging as described above.

Heterogeneous Perchlorate Reduction and Water Sample Analysis. Heterogeneous perchlorate reduction kinetics were measured in continuously stirred aqueous suspensions of Re–Pd/C catalysts. Individual batch reactions were initiated by introducing ClO_4^- from stock solution (0.2 M $NaClO_4$) through the H_2 outlet needle. Suspension aliquots were then periodically collected from the H_2 outlet needle and immediately filtered (0.45-μm cellulose membrane), which quenched any further reaction of ClO_4^-. Reduction of chlorate ($KClO_3$) and chlorite ($NaClO_2$, 80% technical grade) were also conducted using the same approach. Anion concentrations were monitored by ion chromatography with conductivity detection (Dionex ICS-2000). ClO_4^- and ReO_4^- were measured using an IonPac AS16 column (65 mM KOH eluent at 1.2 mL min^{-1} and 30 °C), and ClO_3^-, ClO_2^-, and Cl^- were analyzed on an IonPac AS18 column (32 mM KOH eluent at 1.0 mL min^{-1} flow rate and 30 °C). Total dissolved Re was determined by inductively coupled plasma–optical emission spectrometry (ICP–OES, PerkinElmer Optima 2000DV). Electrospray ionization quadrupole time-of-flight mass spectrometry (ESI–Q–TOF MS, Waters Q–ToF Ultima) analysis was applied to measure dissolved Re complexes and hoz ligand in the water samples.

Catalyst Characterization. Solid catalysts were collected inside the anoxic glovebox from selected batch reactions by vacuum filtration and dried at 110 °C (sand bath). The Re and Pd contents were determined by ICP–OES after a microwave digestion in HNO_3–H_2O_2. The N and Cl contents were determined by CHN and halide analysis. X-ray photoelectron spectroscopy (XPS) was used to characterize the oxidation states of immobilized Re and Pd. To avoid artifacts from air oxidation, dried catalyst powders were loaded onto copper conductive tape inside the anoxic glovebox chamber and transported in an anoxic sample chamber to the X-ray photoelectron spectrometer (Physical Electronics PHI 5400) equipped with a monochromatized Mg Kα source. The sp^2 C 1s peak (284.5 eV) of the carbon support of heterogeneous catalyst or organic ligand phenyl moieties in Re complexes was used for binding energy (BE) normalization. The Re 4f and Pd 3d spectra were fit by constraining the separation of characteristic doublet peaks (2.43 eV for Re, 5.26 eV for Pd) and the ratio of doublet peak areas (4:3 for Re, 3:2 for Pd)[39] using CasaXPS software.

RESULTS

Preparation of $Re(hoz)_2$–Pd/C Catalyst. The oxorhenium complex precursor $Re^V(O)(hoz)_2Cl$ (**3**) was synthesized (Scheme 1) and immobilized on Pd/C using an in situ aqueous

Scheme 1. Synthesis of Hhoz ligand and $Re^V(O)(hoz)_2Cl$

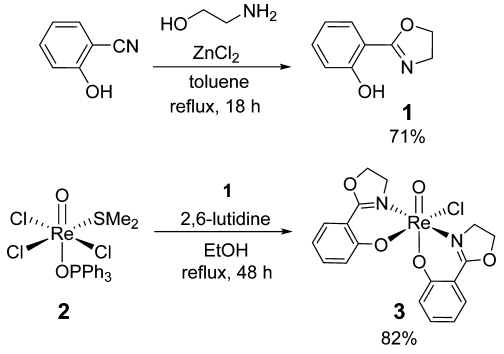

adsorption approach, which was specifically designed to prevent the oxidative decomposition of the active Re species observed previously during catalyst preparation.[34] Micrometer-sized powders of **3** (Supporting Information (SI) Figure S1) were stirred together with Pd/C in water under 1 atm H_2 to prevent exposure to O_2. Over time, the Re complex was taken up by the porous activated carbon support material (Figure 2), yielding the bimetallic $Re(hoz)_2$–Pd/C catalyst. Tests showed that the maximum activity for ClO_4^- reduction by the aqueous $Re(hoz)_2$–Pd/C suspension was observed after allowing **3** and Pd/C to premix for 4 h before introducing ClO_4^- to initiate reaction (Figure 3). This premixing time corresponded to the time required for release of >90% of the coordinated Cl^- from **3** into water. Elemental analysis showed that only traces of Cl remained with the resulting $Re(hoz)_2$–Pd/C catalyst (Table S1), suggesting immobilization of the cationic $[Re^V(O)(hoz)_2]^+$ species. The spontaneous Cl^- release during the aqueous adsorption protocol for Re complex immobilization avoids additional steps required to synthesize the ionic $[Re^V(O)(hoz)_2][OTf]$ or $[Re^V(O)(hoz)_2][B(C_6F_5)_4]$ that have been used in homogeneous catalysis studies.[40,41]

The rate of Re immobilization was limited by the rate of Re dissolution from the solid source of **3** because much longer premixing time was needed to achieve comparable ClO_4^- reduction activity when larger crystals of **3** were used in place of the micrometer-sized powders (SI Figure S1 and Table S2). Incipient wetness impregnation of **3** in Pd/C (conducted under strict anoxic conditions because the immobilized Re species were sensitive to O_2, vide infra) yielded a catalyst showing activity similar to that produced from the in situ aqueous adsorption protocol (SI Table S2), but the latter was used for the remainder of this study because of its simpler preparation procedure.

Catalyst Formulation and ClO_4^- Reduction Activity. Reduction of 1 mM ClO_4^- by $Re(hoz)_2$–Pd/C catalyst with Re

DOI: 10.1021/cs501286w
ACS Catal. 2015, 5, 511–522

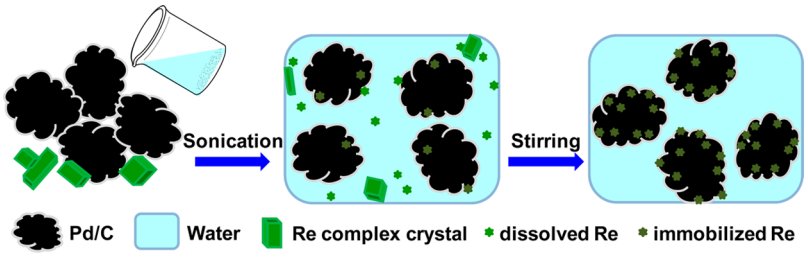

Figure 2. Illustration of Re complex transfer from bulk crystal powders of $Re^{V}(O)(hoz)_2Cl$ (**3**) into Pd/C during the in situ aqueous adsorption process for complex immobilization.

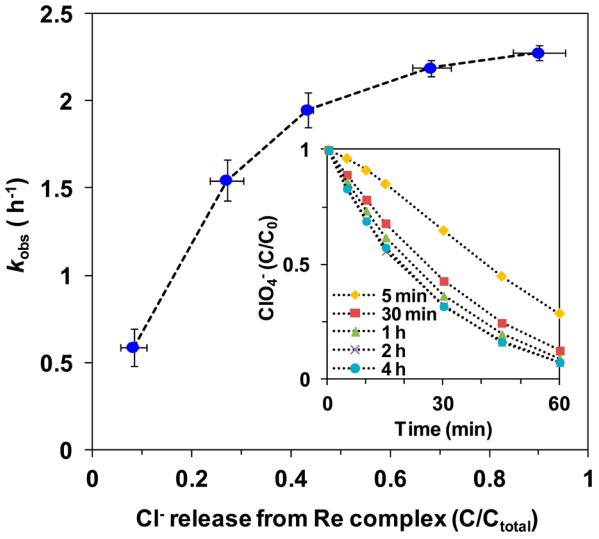

Figure 3. Relationship between the initial rate constant (first-order) for ClO_4^- reduction by $Re(hoz)_2$–Pd/C and Cl^- release to water upon mixing the $Re^{V}(O)(hoz)_2Cl$ precursor (**3**) with Pd/C for different time periods before introducing ClO_4^- to initiate reaction. Inset shows the timecourses for ClO_4^- reduction after different Re complex immobilization times. Reaction conditions: 0.5 g L^{-1} catalyst (nominally 5 wt % Re, 5 wt % Pd), 1 mM ClO_4^-, pH 3, 1 atm H_2, 25 °C.

contents ranging from 1 to 10 wt % (and 5 wt % Pd/C) exhibited pseudo-first-order kinetics. The corresponding estimated OAT turnover number (TON) from ClO_4^- and ClO_x^- intermediates being fully converted to Cl^- at immobilized Re sites ranged from 15 to 150 (0.5 g L^{-1} catalyst to reduce 1 mM ClO_4^-). The ClO_4^- reduction rate constant did not increase linearly with the increasing Re content (SI Table S3, entries 1–4), presumably because the Pd/C surface becomes saturated at higher loadings of the adsorbed Re complex. This trend is similar to that reported for the Re–Pd/C catalyst prepared from ReO_4^- precursor (ReO_x–Pd/C).[36] Apparent catalyst activity improved when increasing amounts of Pd/C were used to immobilize the same mass of Re (SI Table S3, entries 3, 5, and 6), indicating that overall catalyst activity is dependent on both the Pd and Re subcomponents; the 5 wt % Re/5 wt % Pd catalyst exhibited the optimum activity and was used for subsequent experiments. Dissolved H_2 concentration (saturated at 0.8 mM by continuous H_2 sparging)[42] was not a rate-limiting factor, as demonstrated by the linear dependence of rate constants on overall catalyst loadings ranging from 0.125 to 2.0 g L^{-1} (SI Figure S2).

Reactivity of the $Re(hoz)_2$–Pd/C catalyst with ClO_4^- was found to be ~100 times greater than a ReO_x–Pd/C catalyst,[37] ~7 times greater than a 4-dimethylaminopyridine (DMAP)-enhanced ReO_x–Pd/C catalyst,[35] and ~7 times greater than a Re–Pd/C catalyst previously prepared by incipient wetness impregnation of the same $Re(O)(hoz)_2Cl$ precursor complex performed under air (where oxidative decomposition of the

Table 1. Comparison of Catalytic and Stoichiometric Reduction Systems for ClO_4^- in Water

entry	catalyst/reductant	temp	catalyst/reductant loading	pH	rate, k_{obs}, or ClO_4^- conversion[a]	ref
			Heterogeneous Catalysis			
1	$Re(hoz)_2$–Pd/C; H_2[b]	25 °C	0.5 g L^{-1}[c]	3.0	2.49 h^{-1}	
2	Re–Pd/C from $Re(O)(hoz)_2Cl$; H_2[d]	25 °C	0.5 g L^{-1}[c]	3.0	0.316 h^{-1}	34
3	ReO_x–Pd/C; H_2	25 °C	0.5 g L^{-1}[c]	3.0	0.025 h^{-1}	
4	DMAP+ReO_x–Pd/C; H_2	25 °C	0.5 g L^{-1}[c]	3.0	0.318 h^{-1}	
5	hoz+ReO_x–Pd/C; H_2	25 °C	0.5 g L^{-1}[c]	3.0	0.14 h^{-1}	
6	2-Me-oxazoline+ReO_x–Pd/C; H_2	25 °C	0.5 g L^{-1}[c]	3.0	0.017 h^{-1}	
7	78 metal catalysts; H_2	rt	N/A[e]	2.0–9.5	$<10^{-5}$ M h^{-1}	33
			Heterogeneous Stoichiometric Reduction			
8	nano Fe^0	75 °C	20 g L^{-1}	6–8	1.52 mg g_{Fe}^{-1} h^{-1}	16
9	iron fillings	rt	1.25 kg L^{-1}	7.0	66% after 14 days	19
10	Fe powder	150 °C	14.5 g L^{-1}	N/A[e]	85% after 6 h	20
			Homogeneous Stoichiometric Reduction			
11	$FeCl_2$	195 °C	8–16 equiv	4 M HCl	5.233 h^{-1}	17
12	$TiCl_3$/β-alanine (1:3)	50 °C	40 equiv	2.3	1.08 h^{-1}	18

[a]Activity expressions not unified because of the different configurations of the reaction systems. [b]Prepared by aqueous adsorption in this study. [c]Nominally 5 wt % Re and 5 wt % Pd. [d]Prepared by incipient wetness impregnation and dried in air, leading to decomposition of the $Re(O)(hoz)_2Cl$ precursor complex prior to reaction with ClO_4^-. [e]Data not available in the literature.

DOI: 10.1021/cs501286w
ACS Catal. 2015, 5, 511–522

immobilized Re complex was not prevented[34] (Table 1, entries 1–4). In fact, the Re(hoz)$_2$–Pd/C catalyst showed the highest activity (in terms of reaction rate, temperature, reductant type, and dosage) among chemical methods for aqueous ClO_4^- reduction reported to date (e.g., Table 1, entries 7–12).

During the course of batch reactions, a good chlorine mass balance was obtained by summation of ClO_4^- and Cl^- concentrations (SI Figure S3), indicating that ClO_4^- was reduced to Cl^- without accumulation of ClO_x^- intermediates. This is consistent with the observation that ClO_3^- reacts with Re(hoz)$_2$–Pd/C much faster than ClO_4^- (Figure 4). Although

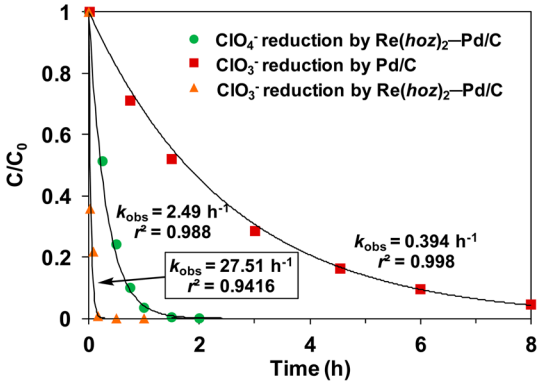

Figure 4. Reduction of ClO_4^- and ClO_3^- with Re(hoz)$_2$–Pd/C and Pd/C (0.5 g L^{-1} catalyst, C_0 = 1 mM, pH 3, 1 atm H_2, 25 °C). Solid lines indicate pseudo-first-order model fits.

ClO_3^- can also be reduced by Pd/C in the absence of Re, the reaction was much faster after immobilization of the Re complex. Similarly, reduction of 1 mM ClO_2^- by the same loading of Pd/C and Re(hoz)$_2$–Pd/C (i.e., equivalent amount of Pd and C) was found to be complete within 120 and 15 s, respectively. These findings suggest that the oxyanions were principally reduced via OAT reactions at the immobilized Re sites rather than by direct hydrogenation at Pd nanoparticle sites.

Re(hoz)$_2$–Pd/C reactivity with ClO_4^- increased with decreasing pH from 6 to 2 (Table 2). A similar pH dependence for Re(hoz)$_2$–Pd/C was observed both when ClO_4^- was added

Table 2. ClO_4^- Reduction by Re(hoz)$_2$–Pd/C at Different pH Conditions

entry[a]	$[ClO_4^-]_0$	pH	$[Cl^-]_{total}$	TON	k_{obs} (h^{-1})[b]
1	1 mM	2	10 mM[c]	30	2.08 ± 0.16
2	1 mM	3	10 mM[d]	30	1.19 ± 0.06
3	1 mM	4	10 mM[d]	30	0.22 ± 0.08
4	1 mM	5	10 mM[d]	30	0.06 ± 0.02
5	1 mM	6[e]	10 mM[d]	30	0.015 ± 0.004
6	10 μM	3	1 mM	0.3	6.98 ± 1.04
7	10 μM	6[e]	1 mM	0.3	0.53 ± 0.01

[a]All reactions measured reduction of ClO_4^- by 0.5 g L^{-1} Re(hoz)$_2$–Pd/C (nominal 5 wt % Re, 5 wt % Pd) at 25 °C under continuous H_2 (1 atm) sparging. Catalysts prepared by in situ adsorption of $Re^V(O)(hoz)_2Cl$ for 4 h. For pH > 3, pH maintained by automatic pH stat with NaOH addition. [b]Determined from pseudo-first-order model fit to the first three half-lives for ClO_4^- reduction. Uncertainties indicate triplicate-averaged standard deviations. [c]From addition of 10 mM HCl. [d]From addition of 1 mM HCl and 9 mM NaCl. [e]1 mM phosphate buffer was used to stabilize pH.

in excess to Re (i.e., TON = 30 for complete reduction; Re redox cycling required to convert an appreciable fraction of the initial ClO_4^- concentration to Cl^-) (Table 2, entries 1–5) and when Re was in excess to ClO_4^- (i.e., TON = 0.3; the immobilized Re completely reduce ClO_4^- to Cl^- without need for rereduction) (Table 2, entries 6, 7). This suggests that the acidity of the aqueous media is mainly limiting the rate of OAT from ClO_4^- to Re rather than the rereduction of oxidized Re products formed following OAT (see Figure 1b). The pH dependence was previously explained by the ancillary hydrogen bonding that facilitates the coordination of aqueous ClO_4^- to the Re center.[35,37] However, as proposed in an early study on homogeneous ClO_4^- reduction with Ti^{III},[43] it is also possible that protonation of the perchlorate oxygens assists the distortion of the bound ClO_4^- in the Re–O–ClO_3 intermediate, thus lowering the LUMO of ClO_4^- and accelerating the electron transfer from Re to Cl.

Reusability of Re(hoz)$_2$–Pd/C catalyst was confirmed by monitoring multiple spikes of 1 mM ClO_4^- to the same batch reactor (0.5 g L^{-1} catalyst; pH 2.7). Rate constants measured from the first five ClO_4^- spikes were sequentially 2.63, 2.00, 2.45, 2.42, and 1.94 h^{-1}, showing only small changes in activity. Activity decreased with additional spikes, dropping to 1.40 h^{-1} by the 10th spike. The observed decrease is attributed to the gradual buildup of Cl^- produced from ClO_4^- spikes in the batch reactor because separate experiments showed a ~50% reduction in the activity of virgin catalysts when initial Cl^- concentration increased from 1 to 10 mM (compare Table 1, entry 1 with Table 2, entry 2).

Metal Speciation in Re(hoz)$_2$–Pd/C Catalyst. XPS was used to characterize the prevailing oxidation states of Pd and Re in the Re(hoz)$_2$–Pd/C catalyst. Both metals exhibit characteristic spin–orbit coupling doublets. Under H_2 atmosphere, Pd was present predominantly as metallic Pd^0 [$3d_{5/2}$ binding energy (BE) 335.0 eV] with a small fraction of Pd^{II} ($3d_{5/2}$ BE 335.7 eV) (Figure 5a). The $4f_{7/2}$ BE (44.2 eV) for powder samples of **3** (measured after a year of storage under air, Figure 5b) matched those reported previously for Re^V coordination compounds.[44] The dominance of Re^V and the trace amount of Re^{VII} ($4f_{7/2}$ BE 46.1 eV) in the sample demonstrate the stability of **3** under O_2. Two oxidation states of Re ($4f_{7/2}$ BE 44.0 and 42.0 eV) were detected in an approximate ratio of 1:1 in the Re(hoz)$_2$–Pd/C catalyst prepared under 1 atm H_2 (Figure 5c). The higher BE is consistent with Re^V, and the lower BE suggests a component with lower Re oxidation state. A previous study on electrochemical reduction of aqueous $[Re^V(O)_2(Py)_4]^+$ (Py = pyridine) reported reduction of the oxo groups to yield $Re^{III}(O)(OH)(Py)_4$ and $[Re^{II}(OH_2)_2(Py)_4]^{2+}$.[45] The reduced Re species in Re(hoz)$_2$–Pd/C most likely results from hydrogenation of the oxo group in the immobilized $[Re^V(O)(hoz)_2]^+$ precursor complex. However, because of the widely ranging and overlapping BE values reported for Re compounds with oxidation states lower than +5,[44] it was necessary to prepare lower oxidation state Re reference compounds with two coordinating hoz ligands to assess the oxidation state in the heterogeneous catalyst.

We synthesized the hoz-coordinated Re^{III} complex to use as an XPS reference standard by oxo group reduction with PPh_3.[29,46,47] After Cl^- abstraction from **3** by AgOTf, heating the cationic $[Re^V(O)(hoz)_2(S)]^+$ complex **4** (S = H_2O or CH_3CN)[40,41] with excess PPh_3 in CH_3CN under reflux yielded $[Re^{III}(hoz)_2(PPh_3)(NCCH_3)][OTf]$ (**5**) and $[Re^{III}(hoz)_2(PPh_3)_2][OTf]$ (**6**) as major and minor products,

DOI: 10.1021/cs501286w
ACS Catal. 2015, 5, 511–522

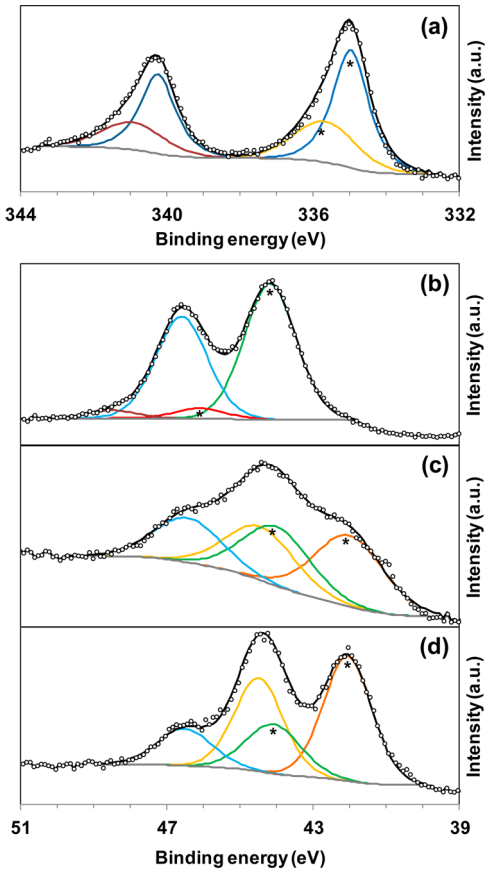

Figure 5. XPS spectra of (a) Pd in $Re(hoz)_2$−Pd/C catalyst, and Re in (b) $Re^{V}(O)(hoz)_2Cl$ (**3**), (c) $Re(hoz)_2$−Pd/C catalyst, and (d) partially air-oxidized $[Re^{III}(hoz)_2(PPh_3)(NCCH_3)][OTf]$ (**5**). Asterisks indicate individual components contributing to fits of the Pd $3d_{5/2}$ or Re $4f_{7/2}$ peaks.

respectively (Scheme 2). Crystal structures of **5** and **6** are shown in Figure 6. ^{1}H−NMR of **5** and **6** shows the wide

Scheme 2. Synthesis of hoz-Coordinated Re^{III} Complexes

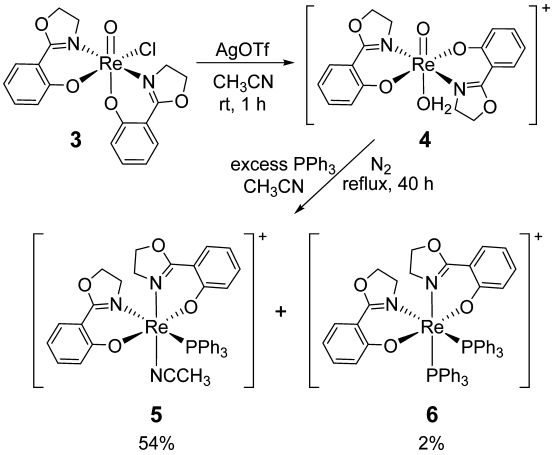

resonance range from −44 to +41 ppm and sharp peaks that are characteristic of paramagnetic Re^{III} species.[46,47] Reflux is necessary for this reduction because room temperature reaction yielded only a $[Re^{V}(O)(hoz)_2(PPh_3)]^+$ in equilibrium with **4** and PPh_3 (see the Supporting Information).

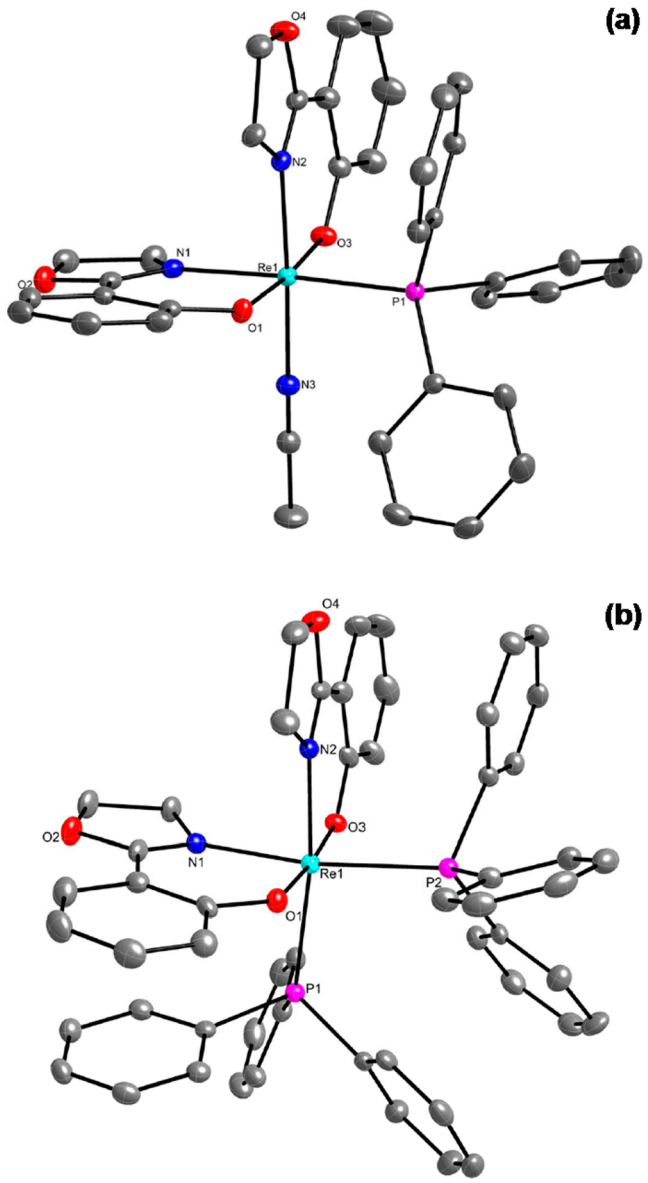

Figure 6. ORTEP diagram (35% probability thermal ellipsoid) of (a) $[Re^{III}(hoz)_2(PPh_3)(NCCH_3)]^+$ (**5**) and (b) $[Re^{III}(hoz)_2(PPh_3)_2]^+$ (**6**). Solvent molecule and anion omitted for clarity.

It was observed that the orange crystals of **5** gradually turned darker when stored on the benchtop. As confirmed by ^{1}H−NMR (vide infra), **5** is slowly oxidized under air to **4**, whereas **6** is much more stable. XPS characterization of **5** after partial air oxidation (Figure 5d) indicates two Re oxidation states ($4f_{7/2}$ BE 44.1 and 42.1 eV), with ΔBE = 2.0 eV, corresponding to hoz-coordinated Re^{V} (**4**) and Re^{III} (**5**), respectively. In comparison, the two Re oxidation states observed in Re-$(hoz)_2$−Pd/C (Figure 5c) also have the same BE separation of 2.0 eV. This agreement suggests that roughly half of the Re immobilized on carbon from the $Re^{V}(O)(hoz)_2Cl$ precursor is reduced to Re^{III}. The approximate 1:1 ratio between Re^{III} and Re^{V} did not change in $Re(hoz)_2$−Pd/C samples after prolonged exposure to H_2, even when heated at 100 °C. The intransigence in Re oxidation states under variable reducing conditions is consistent with local site properties on the Pd/C material controlling the prevailing oxidation state (e.g., direct contact

DOI: 10.1021/cs501286w
ACS Catal. 2015, 5, 511−522

with Pd nanoparticles versus sites on activated carbon distant from Pd).[48]

Reactivity of $Re^{V}(hoz)_2$ and $Re^{III}(hoz)_2$ species with ClO_4^-. The $[Re^{V}(O)(hoz)_2]^+$ complex **4** dissolved in organic solvent has previously been reported to reduce ClO_4^- to Cl^- through a series of OAT reactions.[30,49] In this study, complete oxidation of **4** (10 mM) within 3 min by a stoichiometric concentration of ClO_4^- (2.5 mM, containing 10 mM oxygen atoms for OAT to Re^{V}) in acetonitrile was observed by ^1H NMR. Thus, the high reactivity of ClO_4^- with **4** immobilized on Pd/C serves a possible working mechanism of the heterogeneous catalysis.

To the best of our knowledge, there have been no reports on the reactivity of heterogeneous or homogeneous Re^{III} species with ClO_4^-. Because it is difficult to isolate and measure the specific reactivity of the Re^{III} species immobilized in the heterogeneous catalyst containing both Re^{III} and Re^{V}, we directly measured the homogeneous reactivity of **5** dissolved in CD_3CN with $LiClO_4$. These experiments indicate that **5** cannot react directly with ClO_4^-, but it can react indirectly via intermetal OAT reactions[29] catalyzed by **4** (Scheme 3). The

Scheme 3. Homogeneous Transformation of hoz-Coordinated Re^{III} Complex

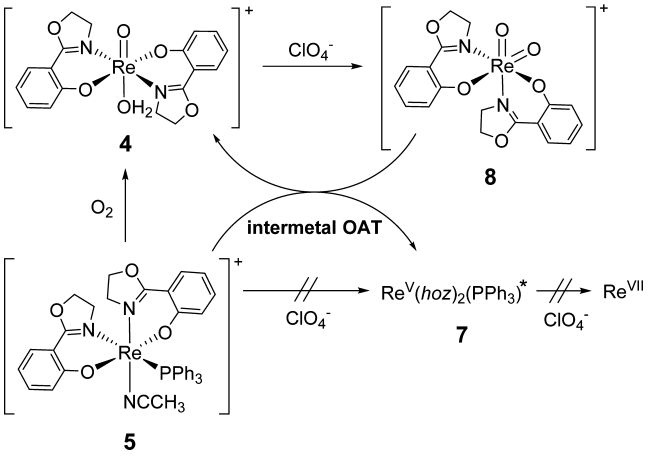

Re^{III} complex was oxidized very slowly when $LiClO_4$ was added to a freshly prepared solution of **5** (which contains only ~0.25 mol % **4** as an impurity) (Figure 7). In comparison, Re^{III} oxidation was rapid when the same experiment was repeated using a comparable solution of **5** that had been aged for 2 days on benchtop (and contained ~6 mol % of **4** due to slow air oxidation of **5** during storage) prior to adding $LiClO_4$. Furthermore, adding 5 mol % of **4** to a freshly prepared solution of **5** promoted similarly rapid oxidation of the latter by $LiClO_4$. These findings are consistent with **4** acting as an OAT catalyst, coupling oxidation of **5** with reduction of ClO_4^-.

Although the observed stoichiometry for Re^{III} oxidation by ClO_4^- indicated predominance of a Re^{V} product rather than Re^{VII}, the structure of the diamagnetic product detected by ^1H NMR (Figure 8a) was not consistent with **3** (Figure 8b), **4** (Figure 8c), or its PPh_3-coordinated $[Re^{V}(O)(hoz)_2(PPh_3)]^+$ structure (Figure 8d). This contrasts with the slow oxidation of **5** by O_2 (air exposure), which yields the latter two products as well as other unidentified species (Figure 8e). Spectral features for the new Re^{V} product **7** (Figure 8a and SI Figure S4) formed by the intermetal OAT (Scheme 3) suggest that the structure contains two asymmetrically coordinated hoz and one tightly

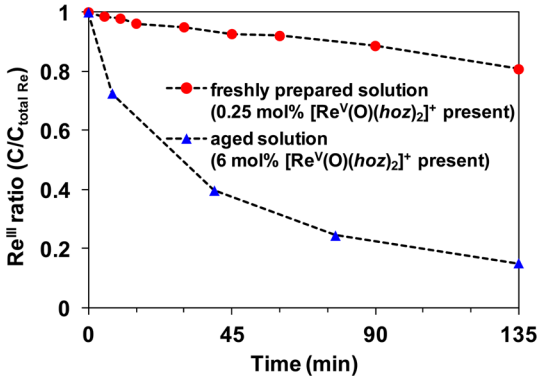

Figure 7. Oxidation of 16 mM $[Re^{III}(hoz)_2(PPh_3)(NCCH_3)]^+$ (**5**) upon 4 mM $LiClO_4$ addition in CD_3CN solutions. Reactions were monitored with ^1H–NMR by quantifying the ratio between the original paramagnetic Re^{III} complex and the diamagnetic Re product upon oxidation.

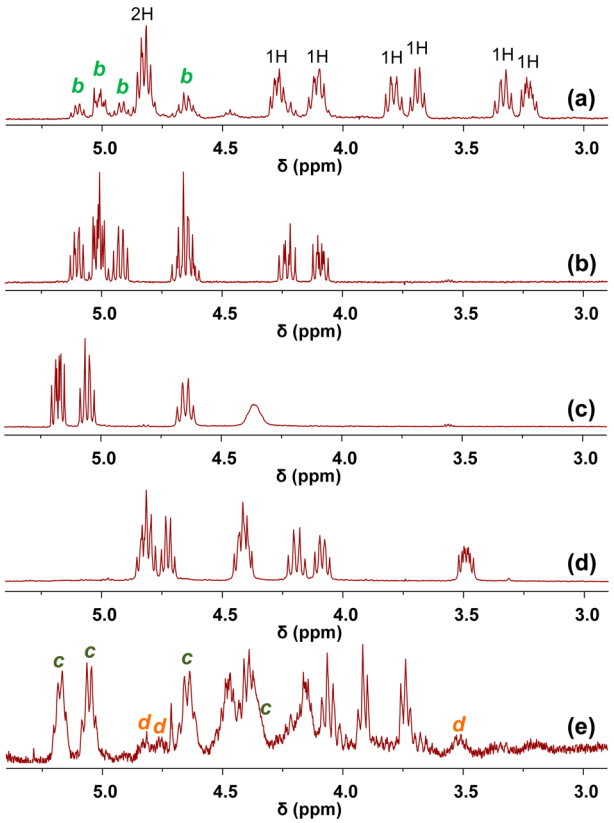

Figure 8. Partial ^1H–NMR (CD_3CN, 500 MHz) spectra of (a) oxidation product of $[Re^{III}(hoz)_2(PPh_3)(NCCH_3)]^+$ (**5**) by ClO_4^-, (b) $Re^{V}(O)(hoz)_2Cl$ (**3**), (c) $[Re^{V}(O)(hoz)_2]^+$ (**4**), (d) $[Re^{V}(O)(hoz)_2(PPh_3)]^+$ in the presence of 20 equiv of PPh_3 and (e) oxidation product of $[Re^{III}(hoz)_2(PPh_3)(NCCH_3)]^+$ by air. Colored and italic letter notes in parts a and e indicate the same resonances found in the corresponding figures.

bound PPh_3 (i.e., not in equilibrium between bound and free PPh_3). Attempts to crystallize **7** were unsuccessful, so we could not obtain the exact structural information. More importantly, though, **7** did not exhibit further reactivity with excess $LiClO_4$ for a period of at least 2 days. In comparison, the $[Re^{V}(O)(hoz)_2(PPh_3)]^+$ in equilibrium with **4** and PPh_3 showed high reactivity with ClO_4^- (see the Supporting Information). Collectively, these results suggest that when the

DOI: 10.1021/cs501286w
ACS Catal. 2015, 5, 511–522

immobilized **4** is further reduced to Re^{III} on the catalyst surface, direct reactivity with ClO_4^- may be lost, although a small portion of the Re^{III} complex may still serve as a reservoir for oxyanion reducing equivalents that can be shuttled through adjacent Re^V species via intermetal OAT processes.

Re Speciation and Reactivity under Variable Conditions. When measuring the reduction of 1 mM ClO_4^- by $Re(hoz)_2$–Pd/C, a low concentration of ReO_4^- (~1% of the initially immobilized Re) was detected transiently in solution. The dissolved ReO_4^- was readsorbed by Pd/C within 1 h, and XPS analysis of the catalyst collected following the reaction (Figure 9a, $4f_{7/2}$ BE 44.0 and 41.9 eV) did not show significant changes from the freshly prepared catalyst (Figure 5c). However, the transient detection of ReO_4^- indicated a small degree of Re complex decomposition.

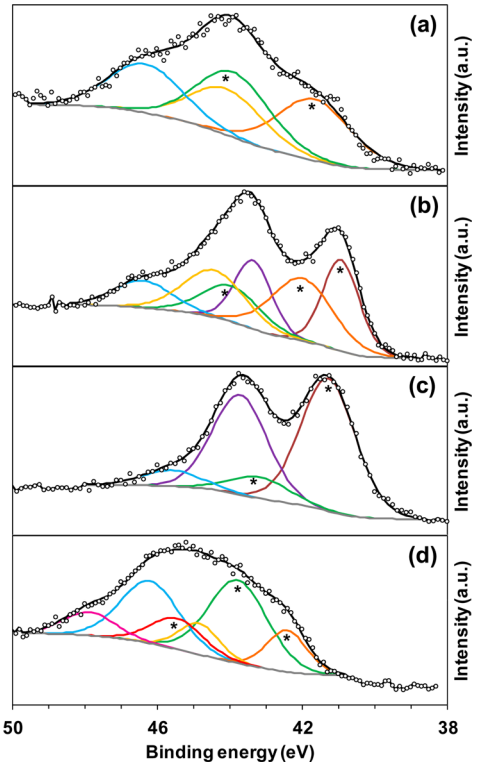

Figure 9. XPS spectra of Re (5 wt %) in (a) $Re(hoz)_2$–Pd/C following reaction with 1 mM ClO_4^-, (b) Re–Pd/C catalyst prepared by reductive immobilization of ReO_4^- in the presence of 2 equiv of hoz, (c) Re–Pd/C catalyst prepared by reductive immobilization of ReO_4^- in the absence of hoz, and (d) $Re(hoz)_2$–Pd/C following air exposure for 10 min. Asterisks indicate individual components contributing to fits of the Re $4f_{7/2}$ peaks.

The in situ aqueous adsorption of ReO_4^- together with 2 equiv of free hoz ligand (simulating a complete decomposition of immobilized Re complex) on Pd/C does not lead to formation of the highly active hoz-coordinated Re^V species. The ClO_4^- reduction activity of this catalyst exhibited only 5-fold higher reactivity than ReO_x–Pd/C prepared from ReO_4^- without hoz ligand added (Table 1, entry 5 vs 3), which was still 16-fold less reactive than $Re(hoz)_2$–Pd/C prepared by aqueous adsorption of the presynthesized complex **3** (Table 1, entry 5 vs 1). XPS characterization of the hoz-amended ReO_x–Pd/C catalyst showed three Re oxidation states (Figure 9b, $4f_{7/2}$ BE 44.0, 42.0, and 40.9 eV) consistent with Re^V, Re^{III}, and Re^I. This differs from both the ReO_x–Pd/C catalyst prepared from ReO_4^- only (Figure 9c, $4f_{7/2}$ BE 43.2 and 41.3 eV) and the $Re(hoz)_2$–Pd/C catalyst prepared from heterogenization of presynthesized **3** (Figure 5c). It follows that if the immobilized $Re(hoz)_2$ structures decompose into ReO_4^- (e.g., by oxidation upon air exposure during conventional incipient wetness catalyst preparation protocols, Table 1, entry 2), the structure and high activity of $Re(hoz)_2$–Pd/C cannot be fully recovered by rereduction of the mixture of ReO_4^- and hoz. Mechanisms and strategies for mitigating the decomposition of immobilized Re complexes are currently under investigation.

DISCUSSION

Re Speciation and Reaction Mechanisms in Heterogeneous $Re(hoz)_2$–Pd/C Catalyst. Transformation of Re species during $Re(hoz)_2$–Pd/C catalyst preparation, catalytic reactions with ClO_4^- and the potential catalyst decomposition are summarized in Figure 10. During catalyst preparation via the in situ aqueous adsorption protocol, Cl^- dissociates from the precursor **3**, and the resulting cationic species **4** absorbs to the activated carbon support (step i) via a combination of hydrophobic and electrostatic interactions; Pd/C carries a negative surface charge in water suspension under H_2 atmosphere.[36] Although both the bulk solid and organic solutions of **3** and **4** are stable in air and an aqueous suspension of **3** showed no significant reactivity with ClO_4^-, dissociation of Cl^- and subsequent dispersion on Pd/C leads to high reactivity of the hoz-coordinated Re species with ClO_4^- and O_2. As shown in Figure 9d, air exposure of the $Re(hoz)_2$–Pd/C powder for only 10 min caused ~20% of the reduced Re species (i.e., Re^{III} and Re^V, $4f_{7/2}$ BE 43.8 and 42.4 eV) to be oxidized to Re^{VII} ($4f_{7/2}$ BE 45.5 eV). Incipient wetness preparation conducted under air, and catalyst storage under air led to the XPS detection of only Re^{VII} and significant ReO_4^- leaching upon mixing in water.[34] Consequently, much lower reactivity with ClO_4^- was observed (Table 1, entry 2 vs 1). However, during the aqueous adsorption protocol, O_2 is eliminated by H_2 sparging and reaction with Pd-activated hydrogen before a significant amount of the Re complex is immobilized in Pd/C. In cases that Re leaching from $Re(hoz)_2$–Pd/C was detected, concentration of total dissolved Re closely matched that of ReO_4^-, indicating that other Re species that might form upon hydrolytic decomposition (e.g., Re complexes still coordinated with hoz structure) are negligible in aqueous solution. This suggests effective sorption of hoz-coordinated Re species to Pd/C in aqueous media, leading to a convenient noncovalent heterogenization[50] of the highly active Re complex. It is also worth pointing out that **3** has a very limited solubility in pure aqueous phase; attempts to dissolve **3** in water by stirring and sonication yielded <10 μM Re in the 0.02-μm filtrate. Furthermore, negligible reaction between ClO_4^- and the suspended powder of **3** was observed, suggesting that **3** alone cannot be used as an effective homogeneous catalyst in aqueous phase. Analysis of total dissolved Re concentration in suspensions of $Re(hoz)_2$–Pd/C prior to reaction with ClO_4^- was only 0.1% of the total immobilized Re. Furthermore, no $[Re(O)(hoz)_2]^+$, ReO_4^-, or $[hoz]^-$ was detected in the water samples taken before and after ClO_4^- reduction catalysis by ESI–MS analysis. Collectively, these findings demonstrate that the catalytic process involves Re complexes immobilized on the carbon support rather than dissolved Re complexes.

The primary catalytic mechanism for ClO_4^- reduction involves redox cycling between Re^V and Re^{VII} complexes, whereas Re^{III} does not participate directly in reactions with

DOI: 10.1021/cs501286w
ACS Catal. 2015, 5, 511–522

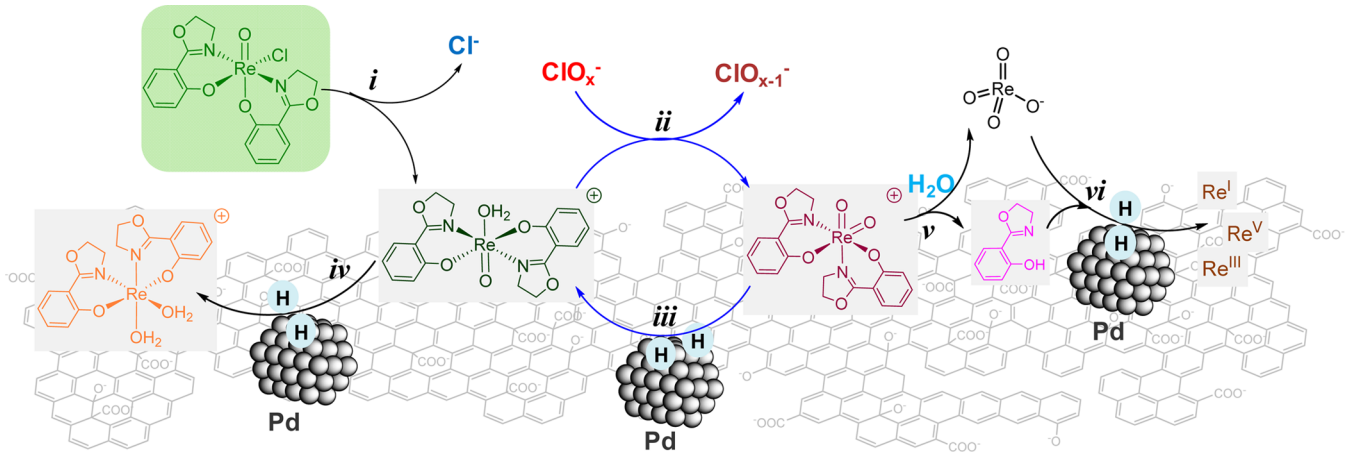

Figure 10. Proposed scheme for immobilization, reaction, and decomposition of hoz-coordinated Re species.

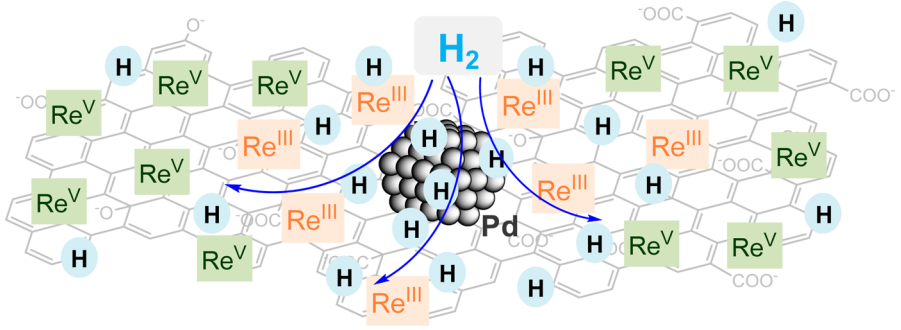

Figure 11. A proposed mechanism of Re distribution in $Re(hoz)_2$–Pd/C catalyst.

ClO_4^-. As illustrated in Figure 10, the immobilized $[Re^V(O)(hoz)_2]^+$ complex accepts a single oxygen atom transferred from ClO_4^- or daughter ClO_x^- products to form $[Re^{VII}(O)_2(hoz)_2]^+$ (step ii), which can then be reduced back to $[Re^V(O)(hoz)_2]^+$ by Pd-activated atomic hydrogen (step iii). About half of the immobilized $[Re^V(O)(hoz)_2]^+$ is further reduced to $[Re^{III}(hoz)_2]^+$ (step iv), which does not have direct reactivity with ClO_4^-. A small fraction (~1%) of immobilized Re complex is susceptible to decomposition into dissolved ReO_4^- (step v), which can be reductively reimmobilized as a mixture of Re^I, Re^{III}, and Re^V surface species (step vi) exhibiting much less reactivity with ClO_4^- than the intact $[Re^V(O)(hoz)_2]^+$ structure.

The system reported here is unique for bimetallic catalysts in that the functioning catalyst combines a single-site reaction center (for OAT from oxyanions) with a metallic nanoparticle (for H_2 activation). This differs from earlier reported catalysts prepared by combining metal complexes with metallic nanoparticles. For example, Rh^I complexes with cyclooctadiene (COD) coordination have been combined with Pd^0 nanoparticles for arene hydrogenation[51−53] and hydrodechlorination of organic environmental contaminants.[54,55] However, during preparation (1 atm H_2, 40 °C) the Rh^I-coordinated ligands are hydrogenated and dissociate, and Rh^I is reduced to metallic Rh^0 as the active catalytic species.[52] The viewpoint for another Rh–Pd/SiO_2 system is that Rh^I is not reduced by Pd-activated hydrogen, but rather, the neighboring Rh^I and Pd^0 synergistically coordinated and then hydrogenated the same arene substrate molecule.[56,57] In comparison, both Re^V and Re^{III} immobilized in $Re(hoz)_2$–Pd/C are still coordinated by hoz ligands. Unlike the ReO_x–Pd/C catalyst, in which ReO_4^- can be immobilized as both monomeric Re^I oxide species directly coordinated to Pd nanoclusters and Re^V oxide clusters on a carbon surface under H_2-reducing conditions,[36,48] coordination of Re with two charged phenolate oxygens prevents further reduction of Re to oxidation states lower than 3+. Re^0 (reported $4f_{7/2}$ BE 39.7 eV) that forms from high-temperature H_2 reduction of Re_2O_7 (reported $4f_{7/2}$ BE 46.7 eV in the same study) in a Re–Pt model system[58] was not detected in any Re–Pd/C samples in this study. Therefore, Re and Pd play distinct roles in the $Re(hoz)_2$–Pd/C catalyst; the immobilized Re^V complexes serve as single-site OAT centers, and Pd^0 nanoparticles serve as sites for H_2 dissociation.

Scanning transmission electron microscopy with energy dispersive X-ray spectroscopy (STEM–EDS) shows that Pd is immobilized on the carbon support as nanometer-sized particles, whereas Re is dispersed more evenly.[34] As a result, facilitation of Re^{V-VII} redox cycling requires reactivity with both Pd-adsorbed atomic hydrogen and hydrogen that spills over to distant sites on the carbon support material.[59−61] We propose that the varying reactivity of different atomic hydrogen species (e.g., adsorbed on Pd versus adsorbed on different carbon support sites) is responsible for the mixture of hoz-coordinated Re^V and Re^{III} species in $Re(hoz)_2$–Pd/C. Whereas rereduction of the OAT product $[Re^{VII}(O)_2(hoz)_2]^+$ to $[Re^V(O)(hoz)_2]^+$ appears to be facilitated by a range of atomic hydrogen species, more reactive atomic hydrogen species (e.g., localized on or in close vicinity of Pd nanoparticles) may reduce $[Re^V(O)(hoz)_2]^+$ to $[Re^{III}(hoz)_2]^+$ (Figure 11). However, another possibility that cannot be ruled out is that the Re^V/Re^{III} distribution is influenced by the local environment of the carbon surface where individual $Re(hoz)_2$ complexes are

DOI: 10.1021/cs501286w
ACS Catal. 2015, 5, 511−522

adsorbed rather than by the distance from Pd^0 sites of H_2 dissociation. Further study is necessary to identify the controlling mechanisms and structural features.

Comparison with Metalloenzymes. Given the bioinspired nature of the hybrid catalyst, some comparison with biological systems is worthwhile. Although $Re(hoz)_2$−Pd/C exhibits promising activity, the metal-normalized ClO_4^- reduction activity reported for a perchlorate reductase separated from *Azospira oryzae* PS was 1700-fold higher (assuming each enzyme molecule contains one MGD-coordinated Mo active site).[62] However, it is worth noting that the isolated metalloenzyme requires more specialized electron donors (e.g., methyl viologen) to maintain the Mo redox cycling[62,63] as a result of separation from the in vivo electron transfer chain involving a complex series of enzymes and electron shuttles. In addition, the isolated enzyme is sensitive to O_2 and slowly loses its activity, even when stored at low temperatures.[62] In comparison, the bioinspired combination of Re sites with Pd nanoparticles directly utilizes H_2 as a simple electron donor, and the synthetic Re precursor **3** is stable under air for extended periods of time (no decomposition after benchtop storage for >2 years). Therefore, the bioinspired $Re(hoz)_2$−Pd/C shows flexibility and promising potential for engineered applications that merits additional study and development.

Mechanistic Implications for Catalyst Design. A potential explanation for the high OAT activity of hoz-coordinated Re^V in comparison to other Re species is an increased electron density on the Re center arising from the resonance of oxazoline O atom p electrons to the C═N bond.[49] This follows previous work showing that ReO_x−Pd/C catalyst activity enhancement upon pyridine coordination depends on the electron-donating strength of the pyridine para substituent: −H < −Me < −OMe < $-NMe_2$.[35] However, no activity enhancement in the ReO_x−Pd/C system was observed when 2-methyl-2-oxazoline (the monodentate moiety of hoz) was added in place of pyridine ligands (Table 1, entry 6 vs 3). Therefore, the phenolate moiety in the hoz structure also plays an important role in Re coordination and OAT activity enhancement. Our lab is now modifying hoz ligand structures seeking to tune Re^V activity by adding electron-donating groups (EDGs) (e.g., −OMe) and electron-withdrawing groups (EWGs) (e.g., −F) to the 4- and 5- position of phenolate moiety to achieve rationally tuned OAT rates.

Additional improvements in catalyst activity could result from further study on the relationship between oxidation state and OAT activity of immobilized Re complexes. Because the more reduced $[Re^{III}(hoz)_2]^+$ has a stronger thermodynamic tendency to be oxidized than $[Re^V(O)(hoz)_2]^+$, the lack of reactivity observed between the Re^{III} complex **5** and ClO_4^- may be attributed to the loss of an oxo group upon reduction of **4**. In the heterogeneous catalyst, incorporation of mono-oxo Re^V complexes with Pd^0 would generate some inactive Re^{III} species under an H_2 atmosphere; however, when another Re−Pd/C catalyst prepared from dioxo $[Re^V(O)_2(Py)_4]^+$ precursors exhibited high activity for ClO_4^- reduction,[35] atomic hydrogen might have activated the immobilized Re by partially reducing the oxo groups in situ (e.g., forming mono-oxo $[Re^{III}(O)(OH_2)(Py)_4]^+$ or other Re species in low oxidation states) because $[Re^V(O)_2(Py)_4]^+$ did not react with ClO_4^- in homogeneous solution[45] and a similar dioxo complex $[Re^V(O)_2(en)_2]^+$ (en = ethylenediamine) did not follow the direct OAT mechanism when reacting with oxyanions.[29,64] Thus, further study on the role of Re oxo groups on OAT reactions could provide insights to facilitate the development of more "metal-economic" heterogeneous catalysts.

Catalyst Application Potential. On the basis of an environmental life cycle assessment study for drinking water ClO_4^- treatment,[65] the high activity of $Re(hoz)_2$−Pd/C catalyst significantly adds to its competitiveness with conventional water treatment technologies (ion exchange and biological reduction). With the long-term goal of developing higher activity and lower cost catalysts, possibly integrating Mo or W complexes (originally identified in reductases and Re neighbors in the Periodic Table)[66] as the active OAT sites, the $Re(hoz)_2$−Pd/C serves as a model for studying the mechanisms of enhanced heterogeneous OAT catalysis. Studies on the performance and stability of $Re(hoz)_2$−Pd/C under relevant source water quality conditions are also in progress.

This study shows that hybridization of OAT metal complexes and hydrogenation metal nanoparticles on activated carbon support could produce novel catalytic properties in aqueous systems that neither metal can achieve alone. Similar to the recent development of complex-semiconductor hybrid photocatalysts,[67−69] coordination metal complexes are anticipated to augment activity and expand the application scope of hydrogenation catalysts. Meanwhile, the electron transfer realized by hydrogen activation and spillover on heterogeneous supports enables convenient utilization of metal complex catalysts for a wide range of aqueous phase reactions. H_2 can be utilized under ambient temperature and pressure as a clean oxygen acceptor alternative to more toxic reagents like sulfides and phosphines. Findings related to Re^V reduction in this study also suggest higher reducing power of Pd-activated hydrogen compared with aryl phosphines (hoz-coordinated Re^V is reduced to Re^{III} by H_2 and Pd/C at room temperature, whereas high temperature was required for Re^V reduction by aryl phosphines). By using similar bimetallic systems, product isolation challenges arising from the use of phosphines (e.g., PPh_3 recovery and $OPPh_3$ removal)[70,71] for OAT reactions in organic transformation might also be circumvented, leading to new synthetic strategies for green chemistry.

CONCLUSION

In pure aqueous phase and at ambient conditions, the heterogeneous catalyst containing immobilized $Re(hoz)_2$ complexes and Pd nanoparticles on activated carbon realizes facile and complete ClO_4^- reduction using H_2 as a clean electron donor (H_2O is the only byproduct). The Re^{V-VII} redox cycle serves as the main catalytic mechanism; however the immobilized Re^V complex could also be hydrogenated to an inactive Re^{III} or to Re^I as a result of the irreversible decomposition of hoz-coordinated structure. Although this bioinspired synthetic catalyst remains less active than isolated metalloenzymes, it has potential advantages in terms of simplicity, tunability, and stability. Performance of the hybrid catalyst and identified mechanistic features of the reactions suggest multiple strategies for further improvement of catalyst activity, and findings reported here demonstrate a promising direction for developing novel hybrid catalysts combining metallic nanoparticles and single-site reactive metal complexes on the same support. Highly active metal complexes, which were initially developed for organic phase catalysis, can thus be integrated into heterogeneous catalysts used for environmental remediation and green chemistry applications.

DOI: 10.1021/cs501286w
ACS Catal. 2015, 5, 511−522

■ ASSOCIATED CONTENT

Supporting Information

The following files are available free of charge on the ACS Publications website at DOI: 10.1021/cs501286w.

Tables S1 to S3; Figures S1 to S4; text and figures providing details on experimental methods (PDF)
Crystallography tables and CIF files for **5** and **6** (CIF)

■ AUTHOR INFORMATION

Corresponding Author

* Phone: +1(217)244-4679. E-mail: strthmnn@illinois.edu.

Present Addresses

[¶]J. Choe: Department of Civil and Environmental Engineering, Stanford University, Stanford, CA 94305
[§]Y. Wang: Department of Civil and Environmental Engineering, University of Wisconsin−Milwaukee, Milwaukee, WI 53211
[⊥]C. Werth: Department of Civil, Architectural and Environmental Engineering, University of Texas at Austin, Austin, TX 78712

Notes

The authors declare no competing financial interest.

■ ACKNOWLEDGMENTS

Financial support was provided by the National Science Foundation (CBET-0730050 and CBET-0746453) and the USEPA Science to Achieve Results Program (Grant No. R835174). D. Wu (Ohio State University), K. Suslick (University of Illinois at Urbana−Champaign), M. Abu-Omar (Purdue University) and S. Liu (Purdue University) are acknowledged for helpful discussions. D. Gray and J. Bertke (University of Illinois at Urbana−Champaign, George L. Clark X-ray Facility & 3M Materials Laboratory) conducted crystallography analysis. Y. Liu (University of Illinois at Urbana−Champaign) conducted optical microscopy characterization. XPS analysis and SEM characterization were conducted at the Frederick Seitz Materials Research Laboratory Central Facilities (University of Illinois at Urbana−Champaign). Three anonymous reviewers provided insightful comments to help improve the presentation of the results in this paper.

■ REFERENCES

(1) United Nations World Water Assessment Programme. *The United Nations World Water Development Report 2014: Water and Energy*; UNESCO: Paris, 2014.
(2) Shannon, M. A.; Bohn, P. W.; Elimelech, M.; Georgiadis, J. G.; Marinas, B. J.; Mayes, A. M. *Nature* **2008**, *452*, 301−310.
(3) Scott, A. *Chem. Eng. News* **2013**, *91* (29), 11−15.
(4) Ainsworth, S. J. *Chem. Eng. News* **2013**, *91* (29), 33−35.
(5) Blount, B. C.; Alwis, K. U.; Jain, R. B.; Solomon, B. L.; Morrow, J. C.; Jackson, W. A. *Environ. Sci. Technol.* **2010**, *44*, 9564−9570.
(6) Parker, D. R.; Seyfferth, A. L.; Reese, B. K. *Environ. Sci. Technol.* **2008**, *42*, 1465−1471.
(7) Wang, Z.; Forsyth, D.; Lau, B. P. Y.; Pelletier, L.; Bronson, R.; Gaertner, D. *J. Agric. Food Chem.* **2009**, *57*, 9250−9255.
(8) Jackson, W. A.; Joseph, P.; Laxman, P.; Tan, K.; Smith, P. N.; Yu, L.; Anderson, T. A. *J. Agric. Food Chem.* **2005**, *53*, 369−373.
(9) Dasgupta, P. K.; Dyke, J. V.; Kirk, A. B.; Jackson, W. A. *Environ. Sci. Technol.* **2006**, *40*, 6608−6614.
(10) Poghosyan, A.; Sturchio, N. C.; Morrison, C. G.; Beloso, A. D.; Guan, Y.; Eiler, J. M.; Jackson, W. A.; Hatzinger, P. B. *Environ. Sci. Technol.* **2014**, *48*, 11146−11153.
(11) Rao, B.; Estrada, N.; McGee, S.; Mangold, J.; Gu, B.; Jackson, W. A. *Environ. Sci. Technol.* **2012**, *46*, 11635−11643.
(12) Greer, M. A.; Goodman, G.; Pleus, R. C.; Greer, S. E. *Environ. Health Perspect.* **2002**, *110*, 927−937.
(13) Coates, J. D.; Achenbach, L. A. *Nat. Rev. Microbiol.* **2004**, *2*, 569−580.
(14) U.S. Environmental Protection Agency. Regulatory Determination on Perchlorate. *Fed. Regist.* **2011**, *76*, 7762−7767.
(15) *Barstow Groundwater Perchlorate Contamination*; California Regional Water Quality Control Board, Lahontan Region: South Lake Tahoe, CA, 2012.
(16) Cao, J.; Elliott, D.; Zhang, W. *J. Nanopart. Res.* **2005**, *7*, 499−506.
(17) Gu, B.; Dong, W.; Brown, G. M.; Cole, D. R. *Environ. Sci. Technol.* **2003**, *37*, 2291−2295.
(18) Wang, C.; Huang, Z.; Lippincott, L.; Meng, X. *J. Hazard. Mater.* **2010**, *175*, 159−164.
(19) Moore, A. M.; De Leon, C. H.; Young, T. M. *Environ. Sci. Technol.* **2003**, *37*, 3189−3198.
(20) Hori, H.; Sakamoto, T.; Tanabe, T.; Kasuya, M.; Chino, A.; Wu, Q.; Kannan, K. *Chemosphere* **2012**, *89*, 737−742.
(21) Bertero, M. G.; Rothery, R. A.; Palak, M.; Hou, C.; Lim, D.; Blasco, F.; Weiner, J. H.; Strynadka, N. C. *Nat. Struct. Mol. Biol.* **2003**, *10*, 681−687.
(22) Schwarz, G.; Mendel, R. R.; Ribbe, M. W. *Nature* **2009**, *460*, 839−847.
(23) Jormakka, M.; Törnroth, S.; Byrne, B.; Iwata, S. *Science* **2002**, *295*, 1863−1868.
(24) Crowell, W. R.; Yost, D. M.; Carter, J. M. *J. Am. Chem. Soc.* **1929**, *51*, 786−794.
(25) Crowell, W. R.; Yost, D. M.; Roberts, J. D. *J. Am. Chem. Soc.* **1940**, *62*, 2176−2178.
(26) Haight, G., Jr; Sager, W. *J. Am. Chem. Soc.* **1952**, *74*, 6056−6059.
(27) Haight, G., Jr *J. Am. Chem. Soc.* **1954**, *76*, 4718−4721.
(28) Abu-Omar, M. M.; Espenson, J. H. *Inorg. Chem.* **1995**, *34*, 6239−6240.
(29) Holm, R. *Chem. Rev.* **1987**, *87*, 1401−1449.
(30) Abu-Omar, M. M.; McPherson, L. D.; Arias, J.; Béreau, V. M. *Angew. Chem., Int. Ed.* **2000**, *39*, 4310−4313.
(31) Bergeron, R. J. *Chem. Rev.* **1984**, *84*, 587−602.
(32) Chaplin, B. P.; Reinhard, M.; Schneider, W. F.; Schüth, C.; Shapley, J. R.; Strathmann, T. J.; Werth, C. J. *Environ. Sci. Technol.* **2012**, *46*, 3655−3670.
(33) Wang, D.; Shah, S. I.; Chen, J.; Huang, C. *Sep. Purif. Technol.* **2008**, *60*, 14−21.
(34) Zhang, Y.; Hurley, K. D.; Shapley, J. R. *Inorg. Chem.* **2011**, *50*, 1534−1543.
(35) Hurley, K. D.; Zhang, Y.; Shapley, J. R. *J. Am. Chem. Soc.* **2009**, *131*, 14172−14173.
(36) Choe, J. K.; Shapley, J. R.; Strathmann, T. J.; Werth, C. J. *Environ. Sci. Technol.* **2010**, *44*, 4716−4721.
(37) Hurley, K. D.; Shapley, J. R. *Environ. Sci. Technol.* **2007**, *41*, 2044−2049.
(38) Liu, J.; Choe, J. K.; Sasnow, Z.; Werth, C. J.; Strathmann, T. J. *Water Res.* **2013**, *47*, 91−101.
(39) Van der Heide, P. *X-ray Photoelectron Spectroscopy: An Introduction to Principles and Practices*; John Wiley & Sons, Inc.: Hoboken, NJ, 2012.
(40) Arias, J.; Newlands, C. R.; Abu-Omar, M. M. *Inorg. Chem.* **2001**, *40*, 2185−2192.
(41) Ison, E. A.; Trivedi, E. R.; Corbin, R. A.; Abu-Omar, M. M. *J. Am. Chem. Soc.* **2005**, *127*, 15374−15375.
(42) Gevantman, L. Solubility of Selected Gases in Water. In *CRC Handbook of Chemistry and Physics*, 95th ed.; Haynes, W. M., Ed.; CRC Press: Boca Raton, FL, 2014; pp 5−149.
(43) Liu, B. Y.; Wagner, P. A.; Earley, J. E. *Inorg. Chem.* **1984**, *23*, 3418−3420.

DOI: 10.1021/cs501286w
ACS Catal. 2015, 5, 511−522

(44) NIST. *X-ray Photoelectron Spectroscopy Database*; NIST: Gathersburg, MD. http://srdata.nist.gov/xps/Default.aspx (accessed Dec 6, 2014).
(45) Pipes, D. W.; Meyer, T. J. *Inorg. Chem.* **1986**, *25*, 3256−3262.
(46) Lane, S. R.; Sisay, N.; Carney, B.; Dannoon, S.; Williams, S.; Engelbrecht, H. P.; Barnes, C. L.; Jurisson, S. S. *Dalton Trans.* **2011**, *40*, 269−276.
(47) Seymore, S. B.; Brown, S. N. *Inorg. Chem.* **2000**, *39*, 325−332.
(48) Choe, J. K.; Boyanov, M. I.; Liu, J.; Kemner, K. M.; Werth, C. J.; Strathmann, T. J. *J. Phys. Chem. C* **2014**, *118*, 11666−11676.
(49) McPherson, L. D.; Drees, M.; Khan, S. I.; Strassner, T.; Abu-Omar, M. M. *Inorg. Chem.* **2004**, *43*, 4036−4050.
(50) Fraile, J. M.; García, J. I.; Mayoral, J. A. *Chem. Rev.* **2009**, *109*, 360−417.
(51) Gao, H.; Angelici, R. J. *J. Am. Chem. Soc.* **1997**, *119*, 6937−6938.
(52) Stanger, K. J.; Tang, Y.; Anderegg, J.; Angelici, R. J. *J. Mol. Catal. A: Chem.* **2003**, *202*, 147−161.
(53) Bianchini, C.; Dal Santo, V.; Meli, A.; Moneti, S.; Moreno, M.; Oberhauser, W.; Psaro, R.; Sordelli, L.; Vizza, F. *Angew. Chem., Int. Ed.* **2003**, *42*, 2636−2639.
(54) Ghattas, A.; Abu-Reziq, R.; Avnir, D.; Blum, J. *Green Chem.* **2003**, *5*, 40−43.
(55) Bovkun, T. T.; Sasson, Y.; Blum, J. *J. Mol. Catal. A: Chem.* **2005**, *242*, 68−73.
(56) Barbaro, P.; Bianchini, C.; Dal Santo, V.; Meli, A.; Moneti, S.; Psaro, R.; Scaffidi, A.; Sordelli, L.; Vizza, F. *J. Am. Chem. Soc.* **2006**, *128*, 7065−7076.
(57) Barbaro, P.; Bianchini, C.; Dal Santo, V.; Meli, A.; Moneti, S.; Pirovano, C.; Psaro, R.; Sordelli, L.; Vizza, F. *Organometallics* **2008**, *27*, 2809−2824.
(58) Tysoe, W.; Zaera, F.; Somorjai, G. *Surf. Sci.* **1988**, *200*, 1−14.
(59) Conner, W. C., Jr; Falconer, J. L. *Chem. Rev.* **1995**, *95*, 759−788.
(60) Prins, R. *Chem. Rev.* **2012**, *112*, 2714−2738.
(61) Rozanov, V. V. e.; Krylov, O. V. *Russ. Chem. Rev.* **1997**, *66*, 107−119.
(62) Hutchison, J. M.; Poust, S. K.; Kumar, M.; Cropek, D. M.; MacAllister, I. E.; Arnett, C. M.; Zilles, J. L. *Environ. Sci. Technol.* **2013**, *47*, 9934−9941.
(63) Okeke, B. C.; Ma, G.; Cheng, Q.; Losi, M. E.; Frankenberger, W. T., Jr *J. Microbiol. Meth.* **2007**, *68*, 69−75.
(64) Kriege, L. B.; Murmann, R. K. *J. Am. Chem. Soc.* **1972**, *94*, 4557−4564.
(65) Choe, J. K.; Mehnert, M. H.; Guest, J. S.; Strathmann, T. J.; Werth, C. J. *Environ. Sci. Technol.* **2013**, *47*, 4644−4652.
(66) Enemark, J. H.; Cooney, J. J. A.; Wang, J. J.; Holm, R. *Chem. Rev.* **2004**, *104*, 1175−1200.
(67) Tran, P. D.; Wong, L. H.; Barber, J.; Loo, J. S. *Energy Environ. Sci.* **2012**, *5*, 5902−5918.
(68) Sato, S.; Morikawa, T.; Saeki, S.; Kajino, T.; Motohiro, T. *Angew. Chem., Int. Ed.* **2010**, *49*, 5101−5105.
(69) Sato, S.; Arai, T.; Morikawa, T.; Uemura, K.; Suzuki, T. M.; Tanaka, H.; Kajino, T. *J. Am. Chem. Soc.* **2011**, *133*, 15240−15243.
(70) Sieber, F.; Wentworth, P.; Toker, J. D.; Wentworth, A. D.; Metz, W. A.; Reed, N. N.; Janda, K. D. *J. Org. Chem.* **1999**, *64*, 5188−5192.
(71) Falchi, A.; Taddei, M. *Org. Lett.* **2000**, *2*, 3429−3431.

NOTE ADDED AFTER ASAP PUBLICATION

This paper was published ASAP on December 22, 2014, with the incorrect Supporting Information PDF. The corrected version was reposted December 23, 2014.

DOI: 10.1021/cs501286w
ACS Catal. 2015, 5, 511−522